Balancing the non-linear rosmarinic acid biosynthetic pathway by modular co-culture

2 engineering

3	Zhenghong Li, Xiaonan Wang, Haoran Zhang
1	Department of Chemical and Biochemical Engineering
5	Rutgers, The State University of New Jersey
5	98 Brett Rd, Piscataway, NJ 08854, USA

7

9

10

11

12

13

14

15

16

17

18

19

20

21

22

23

24

1

8 Abstract

Pathway balancing is a critical and common challenge for microbial biosynthesis using metabolic engineering approaches. Non-linear biosynthetic pathways, such as diverging and converging pathways, are particularly difficult for bioproduction optimization, because they require delicate balancing between all interconnected constituent pathway modules. The emergence of modular co-culture engineering offers a new perspective for biosynthetic pathways modularization and balancing, as the biosynthetic capabilities of individual pathway modules can be coordinated by flexible adjustment of the subpopulation ratio of the co-culture strains carrying the designated modules. This study developed microbial co-cultures composed of multiple metabolically engineered E. coli strains for heterologous biosynthesis of complex natural product rosmarinic acid (RA) whose biosynthesis involves a complex diverging-converging pathway. Our results showed that, compared with the conventional mono-culture strategy, the engineered twostrain co-cultures significantly improved the RA production. Further pathway modularization and balancing in the context of three-strain co-cultures resulted in additional production improvement. Moreover, metabolically engineered co-culture strains utilizing different carbon substrates were recruited to improve the three-strain co-culture stability. The optimized co-culture based on these efforts produced 172 mg/L RA, exhibiting 38-fold biosynthesis improvement over the parent strain

used in mono-culture biosynthesis. The findings of this work demonstrate the strong potentials of modular co-culture engineering for overcoming the challenges of complex natural product biosynthesis involving non-linear pathways.

28

25

26

27

Keyword: microbial biosynthesis; modular co-culture engineering; rosmarinic acid; pathway
 balancing; non-linear biosynthetic pathway

31

32

33

34

35

36

37

38

39

40

41

42

43

44

45

46

47

1. Introduction

Recent advances in metabolic engineering and synthetic biology have greatly facilitated the boom of microbial biosynthesis. A wealth of biomolecules with various industrial values, ranging from simple biofuel compounds to complex natural products, have been successfully produced with outstanding bioproduction performance using engineered microbes. Yet, balancing biosynthetic capabilities between different pathway modules, regardless of the pathway length and complexity, remains a major challenge for microbial bioproduction optimization (Jones et al., 2015). Conventional methods for microbial biosynthesis to a large extent rely on engineering microbial mono-cultures, i.e., cultures composed of only one microbial strain, to accommodate the target biosynthesis pathways. Despite its great success in the past decades, this approach needs to overcome critical technical difficulties to meet the increasing need for biosynthetic pathway optimization. For example, pathway balancing in mono-culture is commonly pursued by adjusting the relative expression strengths of the pathway genes belonging to different pathway modules (Jones et al., 2015). This requires laborious trial-and-error efforts in optimizing the gene copy number, expression promoter strength, and ribosomal binding site, etc., which are limited by available bioengineering tools and often leads to sub-optimal bioproduction performance (Jones et al., 2015; Keasling, 2010; Lee et al., 2012; Yadav et al., 2012). Moreover, the difficulties for pathway balancing increase dramatically when non-linear biosynthesis pathways are involved, as there are much more interaction modes between individual pathway modules and thus complex coordination for balancing is required. Given that a considerable number of biosynthetic pathways for value-added products are non-linear, it is of great significance to develop new pathway balancing methodologies beyond the scope of engineering microbial mono-cultures.

48

49

50

51

52

53

54

55

56

57

58

59

60

61

62

63

64

65

66

67

68

69

70

Engineering microbial co-cultures composed of multiple microbial strains has recently received increasing research interests for applications in microbial biosynthesis (Wang et al., 2017). In particular, modular co-culture engineering, an emerging methodology harnessing the power of microbial co-cultures, has been successfully adapted for biosynthesis of a variety of biochemicals with improved performance (Chen et al., 2018; Jones and Wang, 2018; Zhang and Wang, 2016). In this approach, a target biosynthetic pathway is rationally divided into different modules, each of which is then incorporated into a specialized strain. The consolidation of the recruited strains in one cultivation space constitutes the desired co-culture system. Such a design offers several benefits for microbial biosynthesis, such as metabolic stress reduction, cellular environment diversification, and decrease of undesired pathway module interference. Moreover, the modular nature of this design provides new opportunities for implementation of pathway balancing. Specifically, the biosynthetic capabilities of individual pathway modules can be coordinated by manipulating the subpopulation ratio between the co-culture members harboring the corresponding pathway modules. As such, modular co-culture engineering offers a new perspective to circumvent the limitations of mono-culture engineering for achieving effective pathway balancing.

However, most of the previous studies using microbial co-cultures focused on engineering linear biosynthetic pathways, although attempts has been made towards engineering two-strain co-

cultures for meeting the needs of pathways with converging branches (Liu et al., 2018; Thuan et al., 2018). Despite that linear modularization simplifies and thus facilitates the co-culture engineering efforts, it does not fully unleash the potential of modular co-culture engineering for addressing the challenges associated with complex and non-linear biosynthetic pathways. In fact, the modular nature of microbial co-culture design can be easily utilized for balancing for pathways with complex structures. As a proof of concept, this study utilized modular co-culture engineering strategies for balancing a diverging-converging biosynthetic pathway of complex natural product rosmarinic acid (RA).

RA is a plant-derived natural product belonging to the family of polyphenolic compounds. Structurally, RA is an ester of caffeic acid and salvianic acid A (also named 3, 4-dihydroxyphenyllactic acid). It has been found that RA possesses various important nutraceutical and pharmaceutical values, such as antioxidant, anti-inflammatory, antibacterial, and neuroprotective activities (Kim et al., 2015; Petersen, 2013). It has also been reported that RA could be potentially used to treat cancer due to its anticarcinogenic and anti-tumorigenic activities in animals (Anusuya and Manoharan, 2011; Moon et al., 2010; Paluszczak et al., 2010; Venkatachalam et al., 2013; Xu et al., 2010).

As shown in Fig. 1, the RA biosynthesis involves a non-linear diverging-converging pathway. Two aromatic compounds, caffeic acid (CA) and salvianic acid A (SAA) are two parallel precursors required for the condensation reaction to generate RA. CA can be derived from amino acid tyrosine by two consecutive reactions catalyzed by enzymes tyrosine ammonia lyase (TAL) and 4-hydroxyphenylacetate 3-hydroxylase (HpaBC). SAA is produced from tyrosine pathway intermediate 4-hydroxyphenylpyruvate by two-step enzymatic conversion using 4-hydroxyphenylacetate 3-hydroxylase (HpaBC) and D-lactate dehydrogenase (D-LDH). For the

formation of RA, CA needs to be CoA-activated to form caffeoyl-CoA, which is then combined with SAA through a condensation reaction catalyzed by rosmarinic acid synthase (RAS). The whole RA pathway can be divided into two upstream (CA and SAA) modules and one downstream (RA) module. Notably, both CA and SAA are derived from the tyrosine biosynthetic pathway. As such, they compete against each other for the carbon flux from the same upstream pathway. In the meantime, the CA and SAA precursors need to be produced in even molar quantities so that they can be combined for optimal RA production. Change of the metabolic flux in any of the three modules will generate an interactive impact on the other two modules. Therefore, the RA biosynthesis involves a complex diverging-converging pathway whose balancing is highly challenging.

Heterologous RA biosynthesis has been be achieved using mono-cultures of metabolically engineered *E. coli*. Bloch et al. constructed *E. coli* strains to functionally express selected RA pathway enzymes in vivo. After adjusting the corresponding pathway genes' copy numbers and expression promoters, this study achieved the *de novo* RA biosynthesis with a concentration of 1.8 μM (Bloch and Schmidt - Dannert, 2014). Jiang et al. used a different set of enzymes to establish the RA pathway in *E. coli*. Through feeding exogenous CA, they reported biosynthesis of 130 mg/L RA in the recombinant *E. coli* strain (Jiang et al., 2016). Similar strategy was also adapted to produce several RA analogs through feeding designed pathway precursors (Zhuang et al., 2016). However, the RA biosynthesis in the previous studies either produced low concentrations of RA or relied on the use of exogenous precursors, largely due to undesired imbalance between different pathway modules and low overall metabolic pathway flux. In fact, similar pathway balancing issues were encountered in a recent study for microbial biosynthesis of caffeic acid derived phenethyl esters and amides, which are structurally analogous to RA (Wang et al., 2017).

In the present study, we engineered co-cultures composed of multiple *E. coli* strains to effectively address the challenge of RA pathway balancing. To this end, the pathway was modularized and accommodated in different strains, which allowed for segregation of the parallel upstream CA and SAA modules to minimize their competition for the upstream carbon flux. As such, the diverging-converging RA pathway was simplified to a converging pathway in the context of the co-cultures. Moreover, this design facilitated flexible adjustment of the biosynthetic strengths of three individual modules by manipulating the sub-population sizes of the co-culture members harboring the corresponding pathway modules. Specifically, two-strain and three-strain *E. coli* co-cultures were developed to accommodate the modularized RA pathway for bioproduction optimization, respectively. The employment of the rationally designed *E. coli* co-cultures significantly improved the RA bioproduction performance. Our results demonstrate the great potential of modular co-culture engineering in addressing non-linear biosynthetic pathway balancing and pave the way for its further application in microbial biosynthesis involving complex non-linear biosynthetic pathways.

2. Materials and Methods

2.1 Strains and cultivation medium

E. coli DH5α (New England Biolabs, USA) was adapted for DNA cloning. *E. coli* K12 (DE3), BL21 (DE3), P2H and P2I were utilized as the host strains for the RA production. LB (Luria-Bertani broth) medium was used for cultivation of seed cultures. M9Y medium was used for the RA production by *E. coli*. One liter of M9Y medium contained 1 g of NH₄Cl, 3 g of KH₂PO₄, 6.8 g of Na₂HPO₄, 0.5 g of NaCl, 0.24 g of MgSO₄, 1 mL trace elements, 0.5 g of yeast extract and desired amounts of sugar or sugar mixture. The working concentrations of trace elements were:

 $0.4 \text{ mg/L Na}_2\text{EDTA}$, $0.03 \text{ mg/L H}_3\text{BO}_3$, 1 mg/L thiamine, 0.94 mg/L ZnCl_2 , 0.5 mg/L CoCl_2 , 0.38 mg/L CuCl_2 , 1.6 mg/L MnCl_2 , 3.77 mg/L CaCl_2 , and 3.6 mg/L FeCl_2 . IPTG was added into the medium at a final concentration of 0.5 mM. When needed, the antibiotics were supplemented to the medium to the following final concentrations: 100 µg/mL of ampicillin, 50 µg/mL of kanamycin, 34 µg/mL of chloramphenicol, 50 µg/mL of streptomycin.

2.2 Plasmid construction

140

141

142

143

144

145

146

147

148

149

150

151

152

153

154

155

156

157

158

159

160

161

All strains and plasmids used in this study are summarized in Table 1. The sequences of the PCR primers utilized for cloning are given in Table S1. Restriction enzymes and T4 DNA ligase (New England Biolabs, USA) were used for plasmid construction. d-ldh^{Y52A} (Yao et al., 2013; Zhu et al., 2015) and MoRAS genes (Bloch and Schmidt - Dannert, 2014) were codon-optimized and synthesized by Bio Basic Inc, USA. d- ldhY52A gene was inserted to pET28a and pACYC-Duet plasmids using NdeI and XhoI sites to form pRP1 and pRP9. MoRAS gene was inserted to pET21c and pET28a using NdeI and XhoI sites to form pRP2 and pRP8. Pc4CL gene was PCR amplified from plasmid pCDF-trc-RgTAL- Pc4CL using primers ZLPR1CL and ZLPR2CL, and inserted into pET21c using NdeI and XhoI sites to generate plasmid pRP5. The hpaBC genes were amplified from the BL21(DE3) chromosome using primers ZLPR1HP and ZLPR2HP. The PCR product was digested with NdeI and XhoI and then ligated to pET21c and pET28a treated with the same enzymes to generate plasmids pRP3 and pRP7, respectively. Plasmid pRP4 was constructed by digesting pRP1 with XbaI and XhoI to get the *Lpd-ldh* gene, which was then ligated with pRP3 treated by SpeI and XhoI. Plasmid pRP6 was constructed by digesting pRP2 using XbaI and XhoI sites to get the codon-optimized MoRAS gene, which was ligated with pRP5 treated by SpeI and XhoI.

To construct plasmid pRP10, plasmid pBR322 was used as the template for PCR amplification of the *tetA* gene using primers ZLPR1TA and ZLPR2TA. After NdeI/XhoI digestion of the PCR product and pACYCDuet-1, two fragments were ligated to generate plasmid pRP10. Plasmid pRP11 was constructed by digesting pCDF-trc-*RgTAL* with NcoI/SalI and the resulting fragment was ligated with the NcoI/XhoI treated fragment of plasmid pUC57-PDC-VS. Plasmid pRP12 was constructed by digesting pRP6 with BglII/XhoI and inserting the *pc4CL* and *MoRAS* fragment into BamHI/XhoI treated pCDFDuet-1.

For construction of tyrosine overproduction plasmids, a strong constitutive promoter proD (Davis et al., 2010) and an inducible T7 promoter were used. A previously constructed plasmid pPH0-1 (unpublished data) was adapted for over-expression of aroE, aroL, aroA and aroC genes under the control of a strong constitutive promoter proD (Davis et al., 2010). A DNA fragment containing the aroE, aroL, aroA and aroC genes was isolated from pPH0-1 by HindIII/XhoI and inserted into pACYCDuet-1 treated with the same restriction enzymes to generate pBS3. A DNA fragment containing the genes tyrA^{fbr} and aroG^{fbr} was PCR amplified with primers ZLPR1TA and ZLPR21TA using the E. coli P2H chromosomal DNA as the template. The PCR product was digested with SpeI/HindIII followed by ligation with pPH0-1 treated with the same enzymes to make plasmid pBS2. The PCR product was also digested with Sall/HindIII followed by ligation with pBS3 treated with the same enzymes to make plasmid pBS4. For plasmid pRP13, an aroE fragment was first amplified from plasmid pBA3 using primers ZLPR1AE and ZLPR2AE and cloned to the XbaI/XhoI sites of plasmid pUC57-pdc-VS (Zhang and Stephanopoulos, 2016). The resulting plasmid pUC57-pdc-aroE was digested by XbaI/XhoI to transfer the aroE fragment to plasmid pRP3 treated by SpeI/XhoI, generating plasmid pRP13.

2.3 Cultivation conditions

162

163

164

165

166

167

168

169

170

171

172

173

174

175

176

177

178

179

180

181

182

183

For the monoculture, two-strain co-culture and three-strain co-culture biosynthesis in test tube, the seed cultures were first cultivated overnight at 37 °C in LB medium. The overnight cultures were then centrifuged and re-suspended in fresh M9Y medium. After OD measurement, desired amounts of seed cultures were collected and inoculated into the M9Y medium to reach a total initial OD₆₀₀ of 0.6. IPTG was added at the beginning of the cultivation. To identify the optimal cultivation temperature for RA production, cultures of MRA (for mono-culture), RAU1 and RAD1 (for two-strain co-culture) were grown at 25 °C, 30 °C and 37 °C for 48 hours. To maintain the same initial OD₆₀₀ of 0.6, RAU1 and RAD1 were inoculated to reach OD₆₀₀ of 0.3, respectively (RAU1:RAD1 =1:1). For the co-culture system under other different ratios, the needed initial OD₆₀₀ for individual strains was calculated based on the inoculation ratio. Proper amounts of cell cultures were then added in the M9Y medium to a total OD₆₀₀ of 0.6. After 48 hours of cultivation, samples were taken for HPLC analysis.

For shake flask cultivation, seed cultures of the involved strains were cultivated in LB medium, respectively. After overnight growth, individual cultures were centrifuged and re-suspended in fresh M9Y medium. After the OD measurement, desired amounts of re-suspended cell cultures were added to 100 mL fresh M9Y medium at different ratios to make a total initial OD₆₀₀ of 0.6. The co-culture was then grown at 37 °C for 48 hours. The medium used for the shake flask experiments contained 5 g/L glucose for the CAL2:SAL9:MAM2co-culture and 5 g/L sugar mixtures for the CAL11:SAL11:MAM3 co-culture, respectively. Samples at different time points of the cultivation were taken from the culture for OD measurement, strain-to-strain ratio analysis and HPLC quantification.

2.4 Determination of the strain-to-strain ratio

The strain-to-strain ratio of the three-strain co-culture was analyzed by the combination of a blue-white screening method (Zhang et al., 2015a; Zhang et al., 2015b) and an antibiotic selection method. Specifically in the experiment of using glucose as sole carbon source, 10 μL of the CAL2:SAL9:MAM2 co-culture sample was diluted 10⁵ to 10⁶-fold before being spread onto an LB agar plate containing IPTG, X-Gal, ampicillin, kanamycin and chloramphenicol. After 24 h of incubation, the CAL2 strain carrying the disrupted *lacZ* gene generated white colonies while the SAL9 and MAM2 strains carrying the intact *lacZ* gene generated blue colonies. The numbers of blue and white colonies were counted, respectively. 30 ~40 blue colonies were then individually picked and re-streaked on separate spots on a second plate containing 10 μg/mL tetracycline. The resulting 30~40 re-streaks on the tetracycline plate were incubated overnight at 37 °C. Since MAM2 contained the *tetA* gene and SAL9 did not, only MAM2 could make new colonies on the second plate, which was used to distinguish MAM2 and SAL9. All three co-culture strains' colony numbers were counted separately for calculating their ratio in the co-culture population.

For the CAL11:SAL11:MAM3 co-culture grown on xylose/glucose mixture, CAL11 and MAM3 strains formed white colonies on the IPTG and X-Gal plates, while SAA11 formed blue colonies. After counting the numbers of the blue or white colonies, 30~40 white colonies were restreaked on the tetracycline plates. New colonies on the tetracycline plates represented the MAM3 strain, which was then used to distinguish SAL11 and MAM3. All three co-culture strains' colony numbers were counted separately for calculating their ratio in the co-culture population.

2.5 Production analysis

LC-MS/MS was used for confirmation of the RA biosynthesis. 1 mL cell culture was mixed with 1 mL ethyl acetate by vortex for 30 seconds (10 seconds for three times). The mixture was then centrifuged at 11,000 rpm for 1 min. The supernatant (ethyl acetate phase) was transferred to

a clean Eppendorf tube and air dried overnight. The aired samples were dissolved in 1 mL acetonitrile and injected to Agilent 1100 Series HPLC connected with Thermo-Finigan LTQ Mass-Spectrometer. Samples were run through a Waters C18 column using 90% acetonitrile and 10% water for 20 minutes at a flow rate of 0.6 mL/min. Positive-mode ESI was used for ionization, and MS/MS scanning events were set up for the parent ion mass of RA (361 m/z) using 50% ionization energy for fragmentation.

CA, SAA and RA concentrations were determined by HPLC quantification. Culture samples were first collected and centrifuged at 10,000 rpm for 2 minutes. The supernatant was filtered by 0.45 µm PTFE membrane (VWR, Radnor, PA) before subjected to analysis by Agilent 1100 Series HPLC with Photodiode Array detector. The analysis was performed on a Waters C18 column using acetonitrile (solvent A) and water (solvent B) as the mobile phase at a total flow rate of 0.8 mL/min. The following gradient was utilized for elution: 0 min, 100% solvent B; 7 min, 80% solvent B plus 20% solvent A; 9 min, 100% solvent B. Total elution time is 12 minutes. SAA was measured using absorbance at 280 nm. CA and RA were both measured at 320 nm.

3. Results

3.1 RA biosynthesis by an E. coli mono-culture

The establishment of the RA biosynthetic pathway in *E. coli* involves the utilization of the endogenous tyrosine pathway and a group of heterologous enzymes. To this end, we employed a previously constructed *E. coli* tyrosine overproducing strain P2H as the host strain for monoculture biosynthesis, as this strain was capable of generating a strong tyrosine pathway flux for supporting the RA biosynthesis (Santos, 2010). A codon-optimized gene encoding tyrosine

ammonia lyase (TAL) from *Rhodotorula glutinis* and the *E. coli* native *hpaBC* gene encoding 4-hydroxyphenylacetate 3-hydroxylase were used for converting tyrosine to caffeic acid (CA) (Huang et al., 2013; Lin and Yan, 2012). On the other hand, the tyrosine pathway intermediate 4-hydroxyphenylpyruvate was converted to salvianic acid A (SAA) using the *hpaBC* gene and an engineered *Lactobacillus pentosus d-ldh* gene encoding D-lactate dehydrogenase (Yao et al., 2013). Finally, 4-coumarate:CoA ligase (4CL) from *Petroselinum crispus* (Leonard et al., 2006; Yan et al., 2005) and rosmarinic acid synthase (RAS) from *Melissa officinalis* (Bloch and Schmidt - Dannert, 2014) were recruited to produce RA from precursors CA and SAA (Fig. 1).

All the selected pathway genes were cloned into plasmid vectors and subsequently introduced into *E. coli* for reconstitution of the RA pathway. The resulting strain MRA harboring the entire pathway was grown on 5 g/L glucose as a mono-culture for the RA biosynthesis. As shown in Fig. S1A and S1B, the LC/MS/MS chromatograms and mass spectra of the RA standard and the *E. coli*-produced RA matched well, indicating that the desired RA product was indeed produced by strain MRA. Therefore, the *de novo* RA biosynthesis confirmed the desired activity of the constructed heterologous RA pathway in *E. coli*.

As cultivation temperature is often a key factor determining the growth of engineered microbes and the activities of heterologous enzymes, we investigated the effect of temperature on the RA production. As shown in Fig. 2, higher cultivation temperature was found favorable for the RA biosynthesis. For the constructed *E. coli* MRA mono-culture, the produced RA concentration was improved from 1.3 mg/L to 4.5 mg/L, when the temperature was increased from 25 to 37 °C. The production improvement was largely due to the higher cell density at high cultivation temperature. The findings hereby suggested that the RA pathway enzymes did not require a low

temperature to ensure proper protein folding and enzyme activities, and that 37 °C was an appropriate cultivation temperature for the RA biosynthesis.

3.2 RA biosynthesis by two-strain co-cultures

To apply modular co-culture engineering strategy for the RA biosynthesis, we first constructed a co-culture system that used two *E. coli* strains to accommodate the modularized pathway (Fig. 3A). In this co-culture design, the upstream strain RAU1 was solely responsible for the formation of precursor CA, whereas the downstream strain RAD1 was constructed to contain both the SAA and RA modules. This design allowed each co-culture strain to undertake only a portion of the biosynthetic labor and thus reduced the associated metabolic burden. Moreover, the two strains' ratio inside the co-culture could be manipulated for the purpose of pathway balancing.

RAU1 and RAD1 were first inoculated at 1:1 ratio for cultivation on 5 g/L glucose under different temperatures for the RA biosynthesis. As shown in Fig. 2, the RA biosynthesis by this two-strain co-culture was 83%, 269% and 133% higher than that of the mono-culture under 25, 30, 37 °C, respectively, which clearly demonstrated the power of modular co-culture engineering. Also, 37 °C was found to be the optimal temperature for the RA biosynthesis in the co-culture, which was consistent with the optimal temperature for the MRA mono-culture.

Next, the RA biosynthesis was optimized by changing the initial inoculation ratio of the two co-culture strains, which enabled the flexible adjustment of the biosynthetic strengths between the corresponding pathway modules. As shown in Fig. 3B, the decline of the RAU1:RAD1 inoculation ratio (less RAU1 and more RAD1) resulted in the relatively lower biosynthetic strength of the upstream CA module and higher strength of the SAA and RA modules. With the increase of the inoculation ratio, the corresponding pathway modules' biosynthetic capabilities changed, which resulted in decreased CA concentration and increased SAA concentration. The CA and SAA

provision was best balanced at the inoculation ratio of 3:1, which led to the RA production of 12 mg/L.

The RA biosynthesis was further investigated by adapting additional engineering strategies in the context of the two-strain co-cultures. First, the pathway enzyme responsible for converting *p*-coumaric acid to CA was changed from *E. coli* 4-hydroxyphenylacetate 3-hydroxylase complex HpaBC to *Saccharothrix espanaensis* 4-coumarate 3-hydroxylase Coum3H for better CA biosynthesis (Zhang and Stephanopoulos, 2013). As shown in Fig. 3C, when the new co-culture RAU2:RAD1 harboring the Coum3H from *S. espanaensis* was used, the CA accumulation was improved under all tested inoculation ratios. Moreover, the RA biosynthesis was also increased by this strategy. The SAA concentrations were still comparable to that of the RAU1:RAD1 co-culture, as the SAA provision capability was not changed in the RAD1 strain. The highest RA biosynthesis of 48 mg/L by the RAU2:RAD1 co-culture was 4 times higher than the RAU1:RAD1 co-culture. Notably, the optimal inoculation shifted from 3:1 to 9:1, suggesting that the condition for pathway balancing was changed due to the biosynthesis capability enhancement of the CA module. Coum3H was thus used for the CA module in the following two-strain co-culture studies.

In the second strategy, the *tyrB* gene encoding the tyrosine aminotransferase was deleted from the downstream strain's chromosome. This enzyme is responsible for converting precursor 4-hydroxyphenylpyruvate to tyrosine, and its elimination allowed for stronger metabolic flux towards SAA biosynthesis (Fig. 1). As shown in Fig. 3D, the resulting co-culture RAU2:RAD4 showed higher accumulation of SAA at most inoculation ratios, compared with the RAU2:RAD1 co-culture above. Accordingly, the RA biosynthesis was improved to 60 mg/L after the inoculation ratio optimization. It was also observed that with the inoculation ratio decrease (less inoculum for the upstream strain), the CA accumulation decreased and the SAA accumulation increased. This

finding was consistent with the relative biosynthetic capability change for the corresponding pathway modules. It should be noted that the *tyrB* deletion strategy cannot be employed in the mono-culture design, as it will eliminate the tyrosine provision for the CA module and undermine the overall RA biosynthesis. This situation highlighted an outstanding advantage of modular co-culture engineering for physically segregating pathway modules in separate strains to individually satisfy their different biosynthesis needs, which is challenging to achieve by mono-culture engineering.

In the third strategy, the strain for harboring the SAA+RA module was changed to a strain derived from *E. coli* BL21(DE3) which was commonly used for expression of heterologous enzyme in *E. coli*. Surprisingly, the resulting co-culture RAU2: RAD3 produced merely 20 mg/L RA from 5 g/L glucose after the inoculation ratio optimization (Fig. S2). This RA concentration was much lower than that of the RAU2:RAD1 co-culture, although the CA and SAA accumulation was still similar. This finding indicated that the RA module's activity in BL21(DE3) strain was not well reconstituted. Although the exact reason for this finding is unknown, it is speculated that overly strong expression of several heterologous enzymes in this specialized expression host may generate issues of undesired protein folding and enzyme activity reduction.

Next, we investigated the RA biosynthesis performance when the co-culture design was reconfigured by moving the RA module to the strain harboring the CA module (Fig. S3A). The resulting co-culture strains RAU3 containing the CA and RA modules and RAD2 containing the SAA module were inoculated at different ratios for the RA biosynthesis. As shown in Fig. S3B, RA bioproduction by this RAU3:RAD2 co-culture was dramatically reduced under all inoculation ratios. In fact, for this design of (CA+RA):SAA co-culture, the strain RAU3 harboring the CA and RA module was imposed with excessive metabolic stress, as indicated by the significantly lowered

CA concentrations compared with the previous CA:(SAA+RA) design (Fig. S3B vs Fig. 3C). Therefore, the RA bioproduction reduction was a result of the insufficient supply of CA. On the other hand, although the SAA and CA modules could be relatively balanced by changing the inoculation ratio in the new co-culture, the relative biosynthesis strengths between the CA and RA modules were fixed in strain RAU3. Hence, the lack of the CA and RA module balancing also contributed to the low RA bioproduction in the RAU3:RAD2 co-culture.

3.3 RA biosynthesis was significantly improved using three-strain co-cultures

The RA biosynthesis improvement by the two-strain co-culture design showed the promising prospect of engineering microbial co-cultures for advancing microbial biosynthesis of complex natural products. However, the two-strain co-cultures engineered above were limited to only balancing the biosynthetic strengths between CA and SAA+RA modules or between CA+RA and SAA modules. In order to further unleash the potential of modular co-culture engineering for the RA biosynthesis, three-strain co-cultures were developed for more delicate pathway modularization and balancing. In this system, three engineered *E. coli* strains (upstream *E. coli* 1, upstream *E. coli* 2, and downstream *E. coli*) were recruited for accommodation of the CA, SAA and RA modules, respectively (Fig. 4A). Notably, this design not only further reduced the metabolic stress on each strain, but offered a more flexible way for adjusting the biosynthetic capabilities between all three individual pathway modules.

To this end, we first screened a series of *E. coli* strains to identify the best performers for expressing individual pathway modules. Specifically, 10 *E. coli* strains (combinations of different background strains and the CA module plasmids) were screened for the CA biosynthesis capability. As shown in Fig. 4B, strain CAL2 produced the highest concentration of CA (190 mg/L) from 5 g/L glucose. Similarly, another 10 *E. coli* strains were constructed and screened for the SAA

biosynthesis capability. As shown in Fig. 4C, strain SAL9 was identified to be the highest producer of SAA. Two *E. coli* strains, BL21(DE3) and K12(DE3), with different genotypic characteristics were employed as the host to contain the RA module, which resulted in strains MAM1 and MAM2, respectively. Two three-strain co-cultures CAL2:SAL9:MAM1 and CAL2:SAL9:MAM2 were then constructed to produce RA from glucose.

The interaction between the co-culture members in the three-strain system was more complex and therefore required more sophisticated balancing. To optimize the RA biosynthesis using these new co-cultures, the inoculation ratio between all three constituent strains were adjusted to coordinate the biosynthetic strengths of the three modules. As shown in Fig. 4D, the inoculation ratio change had a strong impact on the RA production. The RA titer fluctuated significantly with the inoculation ratio change. The increase of any strain's inoculation led to the strengthening of corresponding pathway modules and the corresponding production performance change.

For the CAL2:SAL9:MAM1 co-culture, when three strains were inoculated at 1:1:2 ratio, RA was produced at a low titer of 8 mg/L. In contrast, the RA concentration was improved to 74 mg/L at the optimal inoculation ratio of 2:3:1. Also, relatively higher RA production was achieved when the SAA module strain (SAL9) was inoculated at higher ratios. It was therefore indicated that there was strong biosynthetic capabilities imbalance between three pathway modules, which could be compensated through changing the strain-to-strain ratio in the co-culture population.

For the CAL2:SAL9:MAM2 co-culture, the change of the RA production with the inoculation ratio showed different results. RA concentrations were overall higher than CAL2:SAL9:MAM1 at most inoculation ratios, which was consistent with our previous finding that BL21(DE3) strain was not a good expression host for the RA module (Fig. S2). CA and SAA accumulation in the CAL2:SAL9:MAM1 and CAL2:SAL9:MAM2 co-cultures also showed varied profiles, as shown

in Fig. S4. These findings showed that the use of different strains (MAM1 and MAM2) for accommodating the RA module could change the relative biosynthetic strengths between individual pathway modules and thus resulted in varied co-culture biosynthesis behavior. Nonetheless, the highest production of 98 mg/L by the CAL2:SAL9:MAM2 co-culture was 63% higher than the highest production by the two-strain co-cultures (60 mg/L by RAU2:RAD4), indicating that the RA pathway was better balanced in the context of three-strain co-culture.

389

390

391

392

393

394

395

396

397

398

399

400

401

402

403

404

405

406

407

408

409

410

411

The dynamics of the three-strain co-culture biosynthesis was further analyzed by growing CAL2:SAL9:MAM2 on glucose in shake flasks with the inoculation ratio of 2:3:1. As shown in Fig. 5A, the cell density of the co-culture developed with time and reached a plateau at around 8 h. Interestingly, the co-culture population composition showed a highly dynamic change over time. The ratio between co-culture strains' sub-populations started to change immediately after the inoculation. The relatively population size of the SAA module strain SAL9 reduced from 50% to 34% at 8 h. After the co-culture growth entered the stationary phase, this percentage kept declining until it stabilized at around 15% after 18 h. In contrast, the population percentages of the strains harboring the CA and RA modules increased over time and reached the plateaus of 53% and 32%, respectively, at 18 h. These results suggested that the SAL9 was at growth disadvantage when cocultivated with the other two co-culture strains. The delay of the co-culture population stabilization compared with cell density stabilization indicated that the dynamic change of the strain-to-strain ratio and overall cell growth were not synchronized. It was also clearly shown that the SAA module strain was at growth disadvantage in this co-culture, and thus a higher amount of inoculation of this strain was required to compensate its growth decline during the cultivation.

The concentration profiles of CA, SAA and RA was shown in Fig. 5B. Both CA and SAA accumulation was observed throughout the cultivation process. Despite the large difference in the

sub-population sizes of the corresponding strains, CA and SAA concentrations were maintained at comparable levels, which was consistent with the need of even provision of these precursors for the downstream conversion. The RA concentration increased gradually beyond the exponential growth phase, and plateaued in the middle of the stationary phase. The RA production reached 102 mg/L at 48 h. Overall, the concentration profile of CA, SAA and RA suggested that the production of pathway metabolites was not entirely synchronized with the co-culture strains' growth.

3.4 Utilization of mixed carbon substrates to improve co-culture stability and biosynthesis

Next, we attempted to further stabilize the co-culture population composition in order to achieve additional RA biosynthesis improvement. To this end, the co-culture strains were engineered to grow on separate carbon substrates to reduce the growth competition against each other. Specifically, a previously constructed *E. coli* strain P6 with disrupted glucose uptake system (deletion of genes *ptsH*, *ptsI* and *crr*) was used to accommodate the CA and RA modules, respectively, to generate strains CAL11 and MAM3. Meanwhile, *E. coli* strain BX with disabled xylose metabolic pathway (deletion of gene *xylA*) was used to accommodate the SAA module to generate strain SAL11. The CAL11:SAL11:MAM3 co-culture was then cultivated on a sugar mixture of glucose and xylose. In this system, xylose was the preferred carbon substrate for CAL11 and MAM3, whereas glucose was the preferred carbon substrates for SAL11. Such a design allowed us to better manipulate the growth of individual co-culture strains.

For the RA biosynthesis using this strategy, composition of sugar mixture was first optimized. Specifically, four compositions, including xylose to glucose mass ratio of 4:1, 3:2, 2:3 and 4:1 (5 g/L sugar in total), were used for growing the CAL11:SAL11:MAM3 co-culture. As shown in Fig. 6, the RA concentration showed very different profiles at these conditions. Overall, low glucose content (xylose:glucose=4:1, Fig. 6A) only produced low RA biosynthesis, as there was no enough

carbon substrate glucose for supporting the SAA module strain's biosynthetic activity, which had been found to be a potential limiting factor for the RA biosynthesis in one sugar cultivation (Fig. 5A). Similar production was also observed when the xylose:glucose ratio was 2:3 (Fig. 6B). On the other hand, low xylose content (xylose:glucose=1:4, Fig. 6D) was not enough for providing enough carbon substrate for the CA and RA module strains and thus generated sub-optimal production performance, although the highest RA production reached 125 mg/L at the inoculation ratio of 3:2:1.

435

436

437

438

439

440

441

442

443

444

445

446

447

448

449

450

451

452

453

454

455

456

457

In comparison, when 2 g/L xylose and 3 g/L glucose was used for cultivation, the CAL11:SAL11:MAM3 co-culture produced greater than 110 mg/L RA at all tested inoculation ratios (Fig. 6C). At the optimal ratio of 2:1:1, the RA concentration reached 165 mg/L, 1.7-fold higher than the co-culture grown on sole carbon source of 5 g/L glucose. Furthermore, it was found that, although the CA accumulation was relatively stable with the change of the inoculation ratio, the SAA accumulation varied to a large degree (Fig. S4). Low SAA build-up (10 mg/L) at the optimal inoculation ratio of 2:1:1 suggested relatively thorough SAA bioconversion to RA under this condition, although there was still 32 mg/L CA remaining un-converted. It is noteworthy that the optimal inoculation ratio shifted from 2:3:1 for one-sugar cultivation to 2:1:1 for two-sugar cultivation. This suggested that the SAA module strain SAL11 had better growth in the CAL11:SAL11:MAM3 co-culture (as the easy carbon substrate glucose was solely assimilated by SAL11 without interference with the other two strains) and thus reduced the need of high inoculum for growth coordination with the other two module strains. On the other hand, it was shown that when carbon substrate was switched from glucose to xylose (CAL2:SAL9:MAM2 vs CAL11:SAL11:MAM3), the CA and RA module strains were still able to utilize the new carbon substrate xylose for meeting the growth and biosynthesis needs. These results clearly demonstrated

that engineering co-culture strains to grow on separate carbon substrates was a viable strategy to improve their growth compatibility and the overall co-culture biosynthesis performance.

We further investigated the dynamics of the CAL11:SAL11:MAM3 cultivation by analyzing time samples of the co-culture grown in shake flasks. As shown in Fig. 7A, the cell density of the co-culture increased with time and plateaued after 24 h. Compared with the co-culture grown on single sugar glucose, it took longer for the co-culture grown on glucose/xylose mixture to enter the stationary phase. This was because the uptake of xylose was slower and the biomass was accumulated in a lower rate.

The time profiles of the individual strains' sub-population size variation showed different patterns. SAL11 percentage quickly increased from 25% to around 80% within 6 h, and leveled off at around 70% for the rest of the cultivation period. Compared with its low percentage in the one-sugar cultivation (Fig. 5A), the SAA module strain in the two-sugar cultivation showed much better growth profile. This is again due to its better growth on glucose without the competition of the other co-culture strains, which helped to enhance the SAA provision for the pathway and thus contributed to the final RA production improvement. The percentage of CAL11 decreased rapidly after the inoculation, and fluctuated between 10% and 20% toward the end of cultivation. Similar trend was found for MAM3 whose percentage dropped from 25% and stabilized at around 10% after 12 h. These findings clearly showed that the use of the two sugars to support the co-culture strain growth effectively changed the co-culture population composition's dynamic development with time, which in turn generated a new bioproduction behavior different from the one-sugar cultivation case.

The concentration change of CA, SAA and RA is shown in Fig. 7B. It was observed that CA was accumulated to around 60 mg/L at 24 h and stabilized at this level toward the end of cultivation.

In comparison, SAA accumulation was only higher than CA in the first 12 h, but overall it fluctuated in a relatively small range throughout the cultivation. Although SAL11 occupied the majority of the co-culture population, the SAA concentration was similar to what was observed for the one sugar cultivation. This suggested that the two-sugar strategy did not necessarily increase the pool size of the SAA precursor; instead, it improved the carbon flux through SAA (and CA) for the RA biosynthesis. It was also found that RA concentration steadily increased over time until it leveled off at 48 h. 172 mg/L RA was produced at the end of the cultivation. Interestingly, occurrence of the RA biosynthesis was not limited to the exponential phase. In fact, a significantly fraction of the RA bioproduction took place in the stationary phase, which suggested that there was still stable carbon flux going into the RA pathway at this stage. The dynamic analysis of the co-culture cultivation also showed that the strain-to-strain ratio in the co-culture was not necessarily consistent with the ratio between biosynthesis capabilities of the corresponding pathway modules. For example, although CAL11 subpopulation was much smaller than SAL11, the CA and SAA supplies by these two strains were maintained at a comparable level, which facilitated the RA bioproduction optimization. Nonetheless, our results revealed the dynamic behaviors of the co-culture's growth and biosynthesis and validated the rationale of the co-culture design for addressing the needs of non-linear RA biosynthetic pathway.

498

499

500

501

502

503

481

482

483

484

485

486

487

488

489

490

491

492

493

494

495

496

497

4. Discussion

Balancing a non-linear pathway is a critical challenge for microbial biosynthesis studies. For natural products involving complex biosynthetic pathways, such as the diverging-converging RA pathway, balancing multiple interacting modules is particularly difficult. In fact, for the RA biosynthesis, the delicate balance between the precursor CA and SAA modules can be hardly

achieved using the conventional mono-culture approach. First, extensive engineering efforts are needed to even out the biosynthesis strengths of different modules using genetic engineering approaches, such as optimizing the pathway modules' gene copy number, ribosomal binding site, promoter selection, etc. Second, for this non-linear pathway, the CA and SAA modules are competitors (for attracting flux from the same upstream shikimate pathway) and partners (for feeding parallel precursors for the downstream biosynthesis module) at the same time. How to effectively allocate appropriate metabolic resources between all pathway modules to balance their individual needs as well as to support coordinated biosynthesis efforts remains a huge challenge. On top of these issues, the overwhelming metabolic burden associated with complex natural production pathway makes the pathway balancing even more challenging (Wu et al., 2016).

Utilization of microbial co-cultures composed of multiple strains, however, offers an alternative perspective to address these challenges without the limitation associated with the mon-culture approach. In fact, there have been pioneering studies using engineered microbial co-cultures for improving biosynthesis of complex natural products (Chen et al., 2018; Fang et al., 2018; Ganesan et al., 2017; Jones et al., 2017; Jones et al., 2016; Zhou et al., 2015). This study further explored the potential of this co-culture approach for facilitating the RA biosynthesis. To this end, our co-culture design segregated the CA and SAA modules in separate strains and thus eliminated the need of sharing the same upstream shikimate pathway in one strain, which simplified the diverging-converging pathway to a converging pathway and facilitated the pathway balancing. More importantly, using this co-culture design, the biosynthesis capabilities of the separated pathway modules could be easily coordinated through varying the ratio between the strains carrying the corresponding pathway modules. Furthermore, the division of the pathway alleviated

the metabolic stress on each co-culture strain and improved the individual strain's fitness and biosynthesis performance.

Indeed, our results clearly demonstrated that the modular co-culture engineering approach significantly improved the RA biosynthesis. For the two-strain co-cultures, the RA biosynthesis was improved to 60 mg/L, compared with 4.5 mg/L production by the engineered mono-culture. Importantly, biosynthesis coordination between CA and SAA+RA modules, or between CA+RA and SAA modules was achieved through straightforward manipulation of the inoculation ratio of co-culture strains. It is noteworthy that the use of the co-culture design offered the unique opportunity for implementing *tyrB* deletion to enhance the SAA module. This cannot be achieved in the context of mono-culture due to the CA module's reliance on the TyrB enzyme. Therefore, it serves as a great example that the pathway module segregation by modular co-culture engineering carries unparalleled advantages over mono-culture engineering.

The two-strain co-culture approach mainly addressed the imbalance between CA and SAA+RA modules. Further recruitment of the three-strain co-cultures enabled more flexible balancing between all three individual modules. Although CA and SAA compounds needed to be provided at 1:1 molar ratio for the downstream RA formation, the specific biosynthetic strengths of the CA and SAA modules (CA or SAA biosynthesis per cell) were not necessarily equal. As such, the two harboring strains were inoculated at uneven ratios to coordinate the two compounds' supply for the RA bioproduction optimization. In the meantime, the RA module's bioconversion capability also needed to be matched with the provision of the CA and SAA precursors. This was reflected in the optimized inoculation ratio of 2:3:1, which best satisfied the pathway modules' different needs for pathway balancing. Moreover, growing co-culture strains on different carbon substrates further helped coordinate their growth profiles for improving the population stability

and the biosynthesis performance. It should be noted that the number of possible inoculation ratios increases dramatically as more strains are recruited to constitute the co-cultures. For the three-strain co-cultures of this study, we only investigated the production profiles using 9 inoculation ratios, due to the tremendous workload for testing all possible ratios. It is therefore likely that even higher RA biosynthesis may be achieved using other inoculation conditions.

On the other hand, the optimization of the inoculation ratio, either for two-strain or three-strain co-cultures, only determined the initial co-culture population composition to facilitate the coordination of different modules' biosynthesis capabilities without the real-time adjustment during cultivation. Such a pre-set strain-to-strain ratio in fact changed quite dynamically as the co-culture growth developed (Fig. 5A, and Fig. 7B), which could largely influence the maintenance of pathway balancing. More sophisticated population control strategies, such as periodical addition of extra culture of a specific co-culture, may be used to re-set the strain-to-strain ratio to desired levels in the middle of cultivation.

In conclusion, we achieved bioproduction of 172 mg/L RA using a rationally designed three-strain co-culture, which is 38-fold higher than the original mono-culture strain developed in this study. To our knowledge, the RA concentration is the highest among all related studies for *de novo* RA biosynthesis. More broadly, the use of three-strain co-cultures, especially those engineered to grow on sugar mixtures, has not been well explored before. Thus, the associated findings lay a foundation for future studies aiming at using this strategy to balance pathways with converging and/or diverging braches. Hence, the accomplishment of this study marks an important progress towards unleashing the power of modular co-culture engineering for advancing microbial biosynthesis of complex natural products, especially for those involving non-linear pathways.

Acknowledgement

This material is based upon work supported by the National Science Foundation under Grant No. 1706058. This work is also partially supported by startup research funds from Rutgers, The State University of New Jersey. Zhenghong Li is a recipient of the CSC Ph.D. fellowship.

Table 1. The plasmids and strains used in this study

Plasmids	Description	Source
pTrcHis2B	trc promoter, pBR322 ori, Amp ^R	Invitrogen
pET28a	T7 promoter, Kan ^R	Novagen
pET21c	T7 promoter, Amp ^R	Novagen
pACYCDuet-1	double T7 promoters, Cm ^R	Novagen
pRSFDuet-1	double T7 promoters, Kan ^R	Novagen
pCDFDuet-1	double T7 promoters, Sp ^R	Novagen
pBR322	Amp ^R , Tet ^R	Thermo Scientific
pTE2	pET28a carrying the <i>trpE</i> ^{fbr} , <i>aroG</i> ^{fbr} , <i>aroE</i> , <i>aroL</i> , <i>aroA</i> and <i>aroC</i> gene under the control of T7 promoter	Unpublished data
pHACM- rpoA14	a gTME plasmid carrying a mutated alpha subunit of RNA polymerase for enhancing the shikimate pathway	(Santos et al., 2012)
pTrcHis2B-	pTrcHis2B carrying the codon-optimized <i>RgTAL</i> gene	(Zhang and Stephanopoulos,
RgTAL	gene	2013)
pRSF-Coum3H	pRSFDuet-1 carrying the codon-optimized <i>Coum3H</i> gene	(Zhang and Stephanopoulos,
	Coumsii gene	2013)

pCDF-trc-	pCDFDuet-1 carrying the codon-optimized <i>RgTAL</i>	(Zhang and Stephanopoulos,
RgTAL	gene under the control of trc promoter	2013)
		2013)
cELACU	pET28a carrying the <i>E. coli aroE, aroL, aroA, aroC</i> and <i>ubiC</i> genes under the control of the	This study
	constitutive Zymomonas mobilis pyruvate	
	decarboxylase (pdc) promoter	
pBA3	pET28a carrying the E. coli aroE, aroL, aroA,	(Zhang and Stephanopoulos,
	aroC and ubiC genes	2016)
		2010)
pUC57-PDC-	pUC57 carrying the <i>pctV</i> and <i>shiA</i> genes with the	(Zhang and Stephanopoulos,
VS	constitutive <i>Zymomonas mobilis</i> pyruvate decarboxylase promoter	2016)
	decarboxyrase promoter	2010)
pPH0-1	pET28a carrying the aroE, aroL, aroA and aroC	Unpublished data
	genes under the control of the constitutive <i>proD</i>	
	promoter	
pBS2	pET28a carrying the aroE, aroL, aroA, aroC,	This study
	$tyrA^{fbr}$ and $aroG^{fbr}$ genes under the control of the $proD$ promoter	
pBS3	pACYCDuet-1 carrying the <i>aroE</i> , <i>aroL</i> , <i>aroA</i> ,	This study
pB33	aroC genes	This study
pBS4	pACYCDuet-1 carrying the <i>aroE</i> , <i>aroL</i> , <i>aroA</i> ,	This study
	$aroC$, $tyrA^{fbr}$ and $aroG^{fbr}$ genes	
pRP1	pET28a carrying the codon-optimized <i>Lpd-ldh</i>	This study
	gene	
pRP2	pET21c carrying the codon-optimized <i>MoRAS</i>	This study
mDD2	gene	This store.
pRP3	pET28a carrying the <i>hpaBC</i> gene	This study
pRP4	pET28a carrying the <i>hpaBC</i> gene and codon-	This study
	optimized <i>Lpd-ldh</i> gene	
pRP5	pET21c carrying the codon-optimized <i>Pc4CL</i> gene	This study
pRP6	pET21c carrying the codon-optimized <i>Pc4CL</i> and	This study
	MoRAS genes	
pRP7	pET21c carrying the <i>hpaBC</i> genes	This study
pRP8	pET28a carrying the codon-optimized <i>MoRAS</i>	This study
	gene	

pRP9	pAYCYDuet-1 carrying the codon-optimized <i>Lpd-ldh</i> gene	This study
pRP10	pAYCYDuet-1 carrying the <i>tetA</i> gene	This study
pRP11	pUC57 carrying the codon-optimized <i>RgTAL</i> gene under the control of the constitutive <i>Zymomonas mobilis</i> pyruvate decarboxylase promoter	This study
pRP12	pCDFDuet-1 carrying the codon-optimized <i>Pc4CL</i> and <i>MoRAS</i> genes	This study
pRP13	pET28a carrying the <i>hpaBC</i> and a <i>roE</i> genes	This study
Strains	Description	Source
BL21(DE3)	F- ompT hsdS _B (r _B -, m _B -) gal dcm (DE3)	Invitrogen
K12(DE3)	F- lambda- ilvG- rfb-50 rph-1 (DE3)	(Santos, 2010)
BW25113	F-, Δ(araD-araB)567, ΔlacZ4787(::rrnB-3), λ - , rph- 1, Δ(rhaD-rhaB)568, hsdR514	Yale E. coli Genetic Stock Center
JW4014-2	BW25113 tyrB::kan	Yale E. coli Genetic Stock Center
P2	E. coli K12(DE3) $\Delta pheA \Delta tyrR lacZ$:: $P_{LtetO-1}$ - $tyrA^{fbr}aroG^{fbr} tyrR$:: $P_{LtetO-1}$ - $tyrA^{fbr}aroG^{fbr}$	(Santos, 2010)
P2H	P2 hisH(L82R) (DE3)	(Santos, 2010)
P6	P2H ΔptsH ΔptsI Δcrr ΔaroE ΔydiB	(Zhang et al., 2015b)
BX	E. coli BL21(DE3) ΔxylA	(Zhang et al., 2015b)
P2I	P2H Δ <i>tyrB</i>	This study
MRA	P2H carrying pTrcHis2B- <i>RgTAL</i> , pRP4 and pRP12	This study
RAU1	P2H carrying pTrcHis2B-RgTAL and pRP3	This study
RAD1	P2H carrying pRP4 and pRP6	This study
RAU2	P2H carrying pTrcHis2B-RgTAL and pRSF-Coum3H	This study
RAU3	P2H carrying pTrcHis2B- <i>RgTAL</i> , pRSF- <i>Coum3H</i> and pRP12	This study
RAD2	P2H carrying pRP4, pET21c and pCDFDuet-1	This study

RAD3	BL21(DE3) carrying pBS4, pRP4 and pRP6	This study
RAD4	P2I carrying pRP4 and pRP6	This study
CAL1	RAU2 carrying pHACM-rpoA14	This study
CAL2	RAU1 carrying pHACM-rpoA14	This study
CAL3	P2H carrying pCDF-trc- <i>RgTAL</i> and pRSF- Coum3H	This study
CAL4	P2H carrying pCDF-trc-RgTAL and pRP3	This study
CAL5	P2H carrying pRP11 and pRP7	This study
CAL6	BL21(DE3) carrying pBS4, pCDF-trc- <i>Rg</i> TAL and pRP7	This study
CAL7	BL21(DE3) carrying pBS4, pCDF-trc- <i>Rg</i> TAL and pRSF- <i>Coum3H</i>	This study
CAL8	BL21(DE3) carrying pBS4, pTrcHis2B- <i>RgTAL</i> and pRP7	This study
CAL9	BL21(DE3) carrying pBS4, pTrcHis2B- <i>RgTAL</i> and pRSF- <i>Coum3H</i>	This study
CAL10	BL21(DE3) carrying pBS2, pCDF-trc- <i>RgTAL</i> and pRP7	This study
CAL11	P6 carrying pTrcHis2B- <i>RgTAL</i> , pRP13and pHACM-rpoA14	This study
SAL1	P2I carrying pRP9 and pRP7	This study
SAL2	P2H carrying pRP4	This study
SAL3	P2I carrying pRP1 and pRP7	This study
SAL4	P2I carrying pRP4 plasmid	This study
SAL5	P2I carrying pBS3, pRP1 and pRP7	This study
SAL6	P2I carrying pBS4, pRP1 and pRP7	This study
SAL7	P2I carrying pPH0-1, pRP9 and pRP7	This study
SAL8	P2I carrying pBS2, pRP9 and pRP7	This study
SAL9	BL21(DE3) carrying pBS2, pRP9 and pRP7	This study

SAL10	BL21(DE3) carrying pBS4, pRP1 and pRP7	This study
SAL11	BX carrying pBS2, pRP9 and pRP7	This study
MAM1	BL21(DE3) carrying pRP5, pRP8 and pRP10	This study
MAM2	K12(DE3) carrying pRP5, pRP8 and pRP10	This study
MAM3	P6 carrying pRP5, pRP8 and pRP10	This study

Figure caption

Fig. 1 The diverging-converging biosynthetic pathway of rosmarinic acid. The three highlighted constituent modules (CA module, SAA module, and RA module) are responsible for CA, SAA and RA biosynthesis, respectively. TAL: tyrosine ammonia lyase, TyrB: tyrosine aminotransferase, 4CL: 4-coumarate:CoA ligase, HpaBC: 4-hydroxyphenylacetate 3-hydroxylase, D-LDH: D-lactate dehydrogenase, RAS: rosmarinic acid synthase.

Fig. 2 The effect of cultivation temperature on the RA biosynthesis using the mono-culture and co-culture engineering strategies. The mono-culture (MRA) and co-culture (RAU1:RAD1) were grown on 5 g/L glucose. The co-culture strains RAU1 and RAD1 were inoculated at the ratio of 1:1. Error bars represent standard errors of the means for at least three independent experiments.

Fig. 3 The RA biosynthesis using two-strain co-cultures. (A) The schematic of the two-strain co-culture design. The CA module was accommodated in an upstream *E. coli* strain, whereas the SAA and RA modules were accommodated together in a downstream *E. coli* strain. (B) RA

bioproduction by the RAU1:RAD1 co-culture. RAU1 over-expressed TAL and HpaBC. RAD1 over-expressed D-LDH, HpaBC and RAS. (C) RA bioproduction by the RAU2:RAD1 co-culture. For RAU2, HpaBC was replaced by 4-coumarate 3-hydroxylase (Coum3H) from *Saccharothrix espanaensis*. (D) RA bioproduction by the RAU2:RAD4 co-culture. The *tyrB* gene was deleted from the chromosome of the RAD4 strain.

Fig. 4 The RA biosynthesis using three-strain co-cultures grown on glucose. (A) The schematic of the three-strain co-culture design. The CA, SAA and RA modules were accommodated in upstream *E. coli* 1, in upstream *E. coli* 2 and downstream *E. coli*, respectively. (B) Identification of the optimal *E. coli* strain for the CA bioproduction. 10 engineered strains containing only the CA module were screened for the CA biosynthesis capability. (C) Identification of the optimal *E. coli* strain for the SAA bioproduction. 10 engineered strains containing only the SAA module were screened for the SAA biosynthesis capability. (D) The RA bioproduction by the CAL2: SAL9: MAM1 and CAL2: SAL9: MAM2 co-cultures. CAL2 and SAL9 were the optimal strains for the CA and SAA module, respectively. MAM1 and MAM2 were two RA-module-containing strains derived from *E. coli* BL21(DE3) and K12(DE3), respectively.

Fig. 5 The dynamic growth and RA biosynthesis behaviors of three-strain co-culture CAL2:SAL9:MAM2 cultivated in shake flask. (A) The time profiles of the co-culture cell density change and three strains' individual subpopulation percentage change. (B) The time profiles of the CA, SAA, and RA concentrations in the co-culture.

Fig. 6 The RA biosynthesis using the CAL11:SAL11:MAM3 co-culture grown on sugar mixtures with xylose:glucose ratio of (A) 4:1, (B) 3:2, (C) 2:3 and (D) 1:4. The three constituent strains were inoculated at specified ratios.

623

620

621

622

- Fig. 7 The dynamic growth and RA biosynthesis behaviors of the CAL11:SAL11:MAM3 co-
- culture cultivated in shake flask. 2 g/L xylose and 3 g/L glucose was used as the carbon source.
- 626 (A) The time profiles of co-culture cell density change and three strains' individual subpopulation
- percentage change. (B) The time profiles of the CA, SAA, and RA concentrations in the co-culture.

628

629

Reference

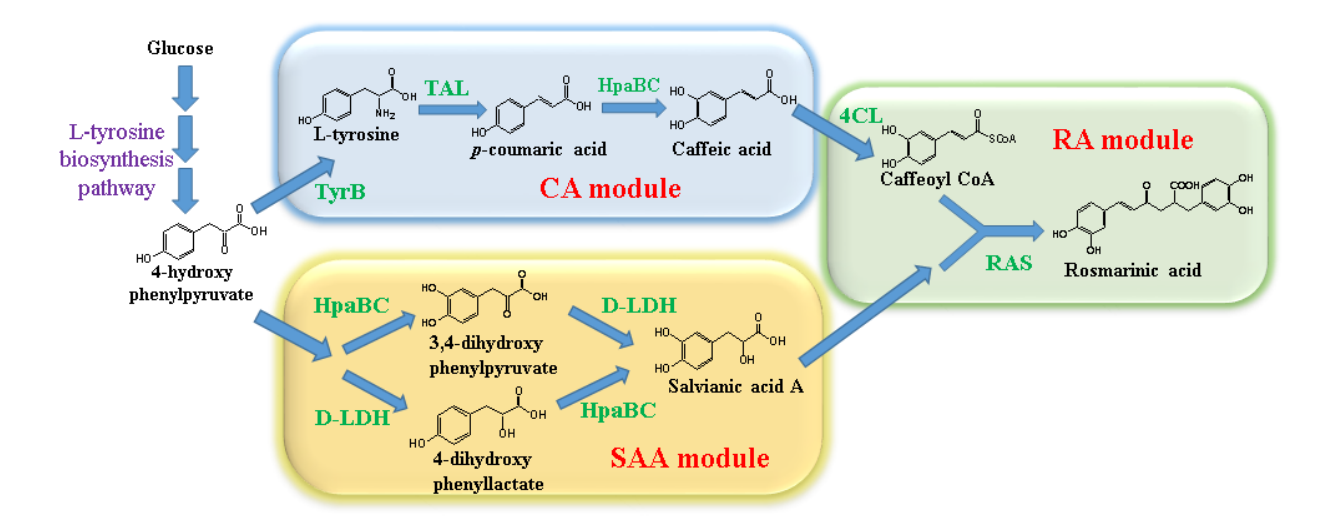
- Anusuya, C., Manoharan, S., 2011. Antitumor initiating potential of rosmarinic acid in 7, 12-
- dimethylbenz (a) anthracene-induced hamster buccal pouch carcinogenesis. Journal of
- Environmental Pathology, Toxicology and Oncology. 30.
- Bloch, S. E., Schmidt-Dannert, C., 2014. Construction of a chimeric biosynthetic pathway for the
- de novo biosynthesis of rosmarinic acid in Escherichia coli. ChemBioChem. 15, 2393-2401.
- 635 Chen, T., Zhou, Y., Lu, Y., Zhang, H., 2018. Advances in heterologous biosynthesis of plant and
- fungal natural products by modular co-culture engineering. Biotechnology letters. 1-8.
- Davis, J. H., Rubin, A. J., Sauer, R. T., 2010. Design, construction and characterization of a set of
- insulated bacterial promoters. Nucleic acids research. 39, 1131-1141.
- Fang, Z., Jones, J. A., Zhou, J., Koffas, M. A. G., 2018. Engineering Escherichia coli co-cultures
- for production of curcuminoids from glucose. Biotechnology Journal. 13, 1700576.
- Ganesan, V., Li, Z., Wang, X., Zhang, H., 2017. Heterologous biosynthesis of natural product
- naringenin by co-culture engineering. Synthetic and systems biotechnology. 2, 236-242.
- Huang, Q., Lin, Y., Yan, Y., 2013. Caffeic acid production enhancement by engineering a
- phenylalanine over-producing Escherichia coli strain. Biotechnology and bioengineering.
- 645 110**,** 3188-3196.

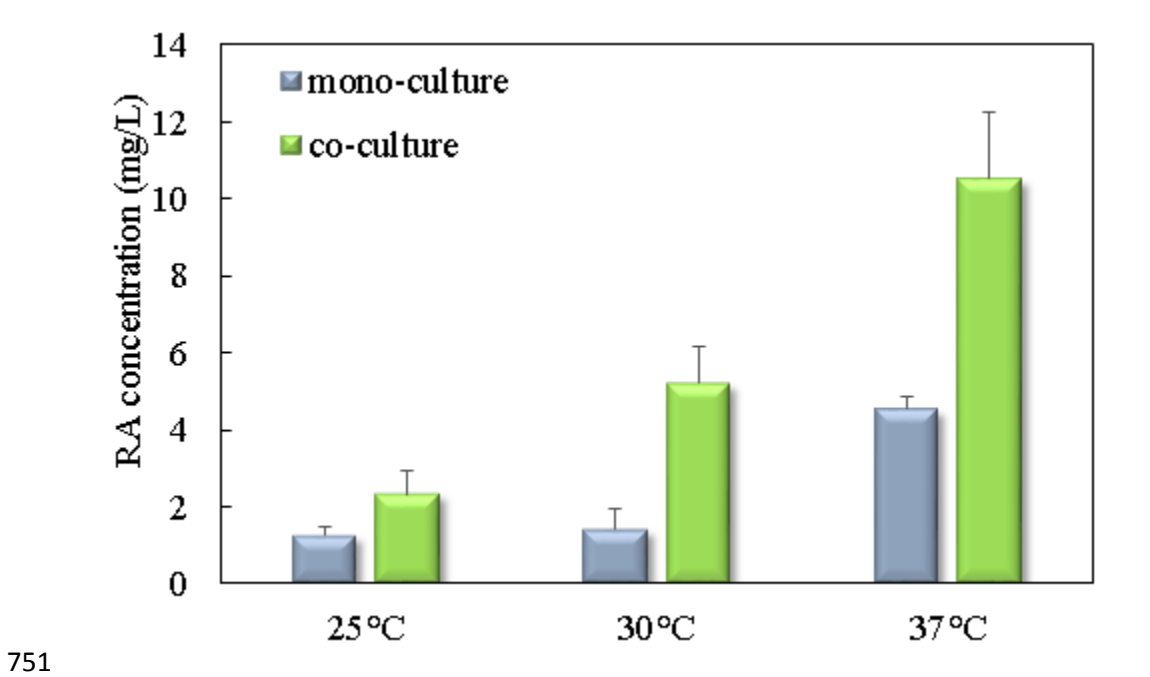
- Jiang, J., Bi, H., Zhuang, Y., Liu, S., Liu, T., Ma, Y., 2016. Engineered synthesis of rosmarinic
- acid in Escherichia coli resulting production of a new intermediate, caffeoyl-phenyllactate.
- Biotechnology letters. 38, 81-88.
- Jones, J. A., Toparlak, Ö. D., Koffas, M. A., 2015. Metabolic pathway balancing and its role in the
- production of biofuels and chemicals. Current Opinion in Biotechnology. 33, 52-59.
- Jones, J. A., Vernacchio, V. R., Collins, S. M., Shirke, A. N., Xiu, Y., Englaender, J. A., Cress, B.
- F., McCutcheon, C. C., Linhardt, R. J., Gross, R. A., Koffas, M. A. G., 2017. Complete
- biosynthesis of anthocyanins using E. coli polycultures. MBio. 8, e00621-17.
- Jones, J. A., Vernacchio, V. R., Sinkoe, A. L., Collins, S. M., Ibrahim, M. H., Lachance, D. M.,
- Hahn, J., Koffas, M. A., 2016. Experimental and computational optimization of an
- Escherichia coli co-culture for the efficient production of flavonoids. Metabolic
- engineering. 35, 55-63.
- Jones, J. A., Wang, X., 2018. Use of bacterial co-cultures for the efficient production of chemicals.
- 659 Current opinion in biotechnology. 53, 33-38.
- Keasling, J. D., 2010. Manufacturing molecules through metabolic engineering. Science. 330,
- 661 1355-1358.
- Kim, G.-D., Park, Y. S., Jin, Y.-H., Park, C.-S., 2015. Production and applications of rosmarinic
- acid and structurally related compounds. Applied microbiology and biotechnology. 99,
- 664 2083-2092.
- Lee, J. W., Na, D., Park, J. M., Lee, J., Choi, S., Lee, S. Y., 2012. Systems metabolic engineering
- of microorganisms for natural and non-natural chemicals. Nature chemical biology. 8, 536.
- Leonard, E., Chemler, J., Lim, K. H., Koffas, M. A., 2006. Expression of a soluble flavone
- synthase allows the biosynthesis of phytoestrogen derivatives in Escherichia coli. Applied
- Microbiology and Biotechnology. 70, 85-91
- 670 Lin, Y., Yan, Y., 2012. Biosynthesis of caffeic acid in Escherichia coli using its endogenous
- hydroxylase complex. Microbial cell factories. 11, 42.
- 672 Liu, X., Li, X.-B., Jiang, J., Liu, Z.-N., Qiao, B., Li, F.-F., Cheng, J.-S., Sun, X., Yuan, Y.-J., Qiao,
- J., 2018. Convergent engineering of syntrophic Escherichia coli coculture for efficient
- production of glycosides. Metabolic engineering. 47, 243-253.

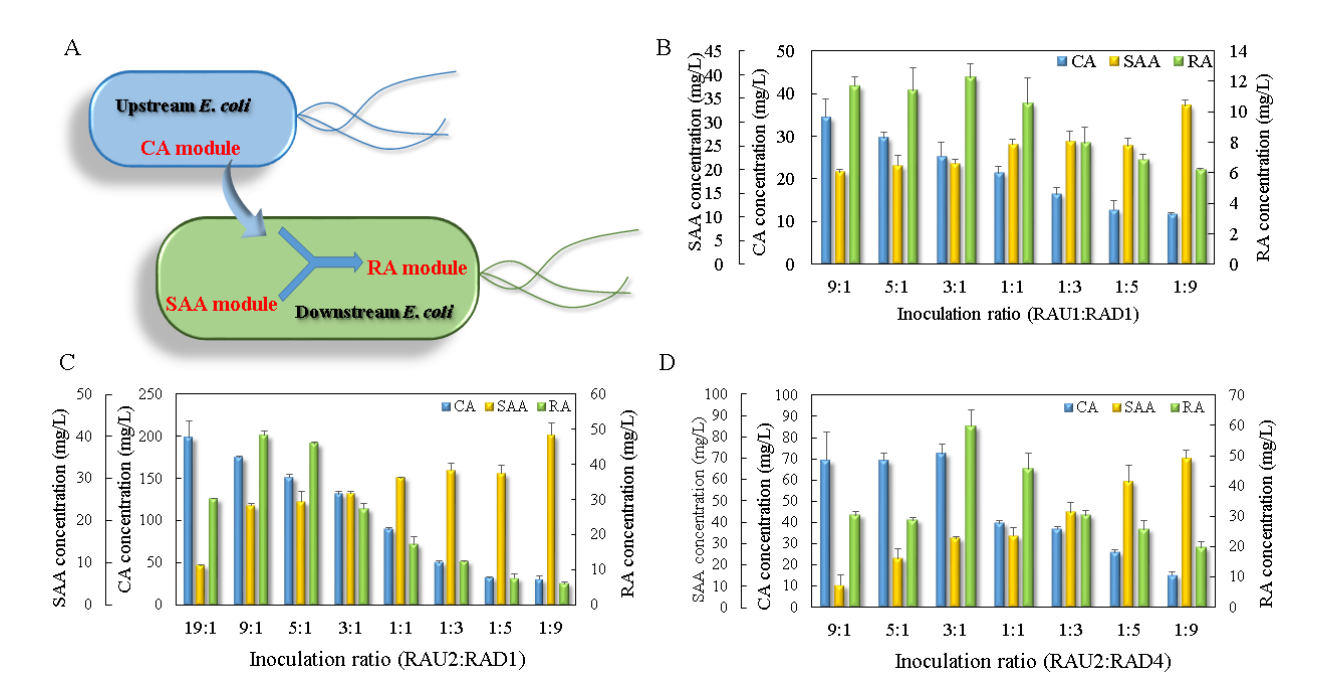
- Moon, D.-O., Kim, M.-O., Lee, J.-D., Choi, Y. H., Kim, G.-Y., 2010. Rosmarinic acid sensitizes
- cell death through suppression of TNF-α-induced NF-κB activation and ROS generation
- in human leukemia U937 cells. Cancer Letters. 288, 183-191.
- Paluszczak, J., Krajka-Kuźniak, V., Baer-Dubowska, W., 2010. The effect of dietary polyphenols
- on the epigenetic regulation of gene expression in MCF7 breast cancer cells. Toxicology
- letters. 192, 119-125.
- Petersen, M., 2013. Rosmarinic acid: new aspects. Phytochemistry Reviews. 12, 207-227.
- Santos, C. N. S., Combinatorial search strategies for the metabolic engineering of microorganisms.
- Massachusetts Institute of Technology, 2010.
- Santos, C. N. S., Koffas, M., Stephanopoulos, G., 2011. Optimization of a heterologous pathway
- for the production of flavonoids from glucose. Metabolic engineering. 13, 392-400.
- Santos, C. N. S., Xiao, W., Stephanopoulos, G., 2012. Rational, combinatorial, and genomic
- approaches for engineering L-tyrosine production in Escherichia coli. Proceedings of the
- 688 National Academy of Sciences. 109, 13538-13543.
- Thuan, N. H., Chaudhary, A. K., Van Cuong, D., Cuong, N. X., 2018. Engineering co-culture
- system for production of apigetrin in Escherichia coli. Journal of Industrial Microbiology
- & Biotechnology. 45, 175-185. Venkatachalam, K., Gunasekaran, S., Jesudoss, V. A. S.,
- Namasivayam, N., 2013. The effect of rosmarinic acid on 1, 2-dimethylhydrazine induced
- colon carcinogenesis. Experimental and Toxicologic Pathology. 65, 409-418.
- Wang, J., Mahajani, M., Jackson, S. L., Yang, Y., Chen, M., Ferreira, E. M., Lin, Y., Yan, Y.,
- 695 2017. Engineering a bacterial platform for total biosynthesis of caffeic acid derived
- 696 phenethyl esters and amides. Metabolic engineering. 44, 89-99.
- 697 Wu, G., Yan, Q., Jones, J. A., Tang, Y. J., Fong, S. S., Koffas, M.A.G., 2016. Metabolic Burden:
- Cornerstones in Synthetic Biology and Metabolic Engineering Applications. Trends in
- 699 Biotechnology. 34, 652-664.
- Xu, Y., Jiang, Z., Ji, G., Liu, J., 2010. Inhibition of bone metastasis from breast carcinoma by
- rosmarinic acid. Planta medica. 76, 956-962.
- Yadav, V. G., De Mey, M., Lim, C. G., Ajikumar, P. K., Stephanopoulos, G., 2012. The future of
- metabolic engineering and synthetic biology: towards a systematic practice. Metabolic
- 704 engineering. 14, 233-241.

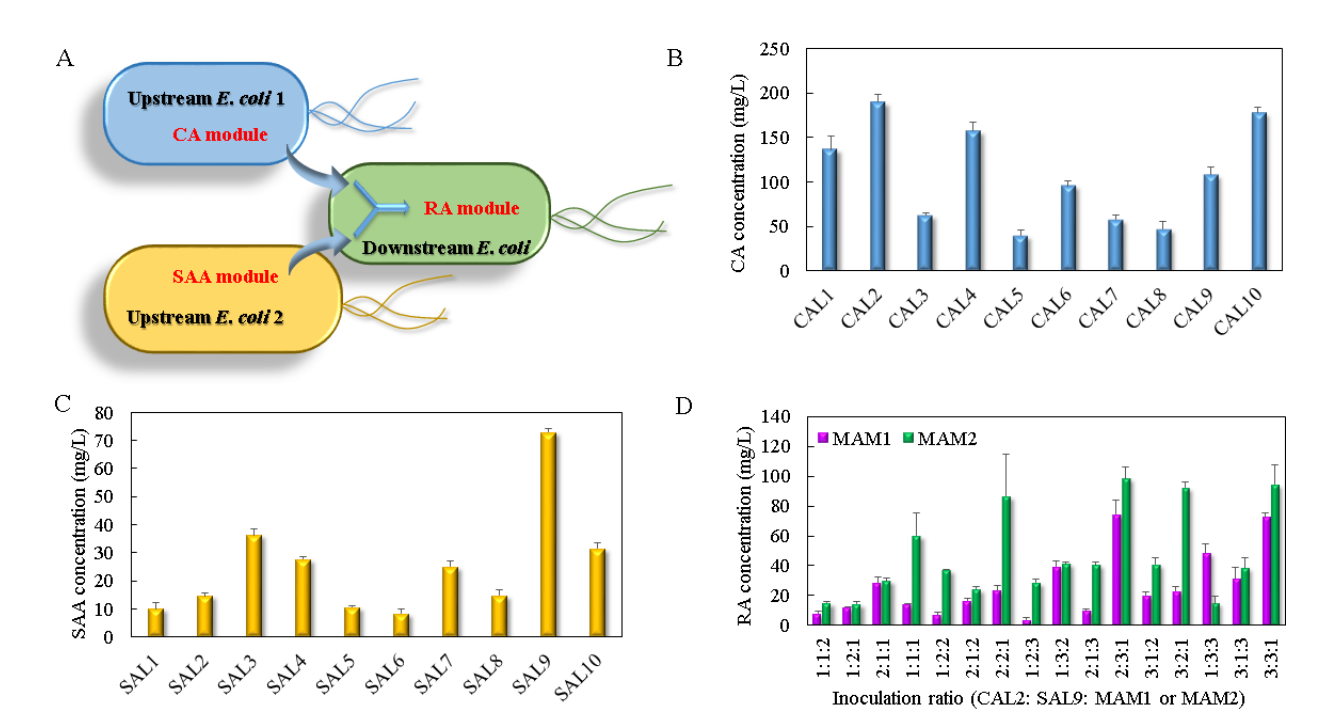
- Yan, Y., Kohli, A., Koffas. M. A., 2005. Biosynthesis of natural flavanones in Saccharomyces
- cerevisiae. Applied and Environmental Microbiology. 71, 5610-5613. Yao, Y.-F., Wang,
- 707 C.-S., Qiao, J., Zhao, G.-R., 2013. Metabolic engineering of Escherichia coli for production
- of salvianic acid A via an artificial biosynthetic pathway. Metabolic engineering. 19, 79-
- 709 87.
- 710 Zhang, H., Li, Z., Pereira, B., Stephanopoulos, G., 2015a. Engineering E. coli-E. coli cocultures
- for production of muconic acid from glycerol. Microbial cell factories. 14, 134.
- 712 Zhang, H., Pereira, B., Li, Z., Stephanopoulos, G., 2015b. Engineering Escherichia coli coculture
- systems for the production of biochemical products. Proceedings of the National Academy
- of Sciences. 201506781.
- 715 Zhang, H., Stephanopoulos, G., 2013. Engineering E. coli for caffeic acid biosynthesis from
- renewable sugars. Applied microbiology and biotechnology. 97, 3333-3341.
- 717 Zhang, H., Stephanopoulos, G., 2016. Co-culture engineering for microbial biosynthesis of 3-
- amino-benzoic acid in Escherichia coli. Biotechnology journal. 11, 981-987.
- 719 Zhang, H., Wang, X., 2016. Modular co-culture engineering, a new approach for metabolic
- engineering. Metabolic engineering. 37, 114-121.
- 721 Zhou, K., Qiao, K., Edgar, S., Stephanopoulos, G., 2015. Distributing a metabolic pathway among
- a microbial consortium enhances production of natural products. Nature biotechnology. 33,
- 723 377.
- 724 Zhu, Y., Hu, F., Zhu, Y., Wang, L., Qi, B., 2015. Enhancement of phenyllactic acid biosynthesis
- by recognition site replacement of D-lactate dehydrogenase from Lactobacillus pentosus.
- 726 Biotechnology letters. 37, 1233-1241.
- Zhuang, Y., Jiang, J., Bi, H., Yin, H., Liu, S., Liu, T., 2016. Synthesis of rosmarinic acid analogues
- in Escherichia coli. Biotechnology letters. 38, 619-627.

Figure 1

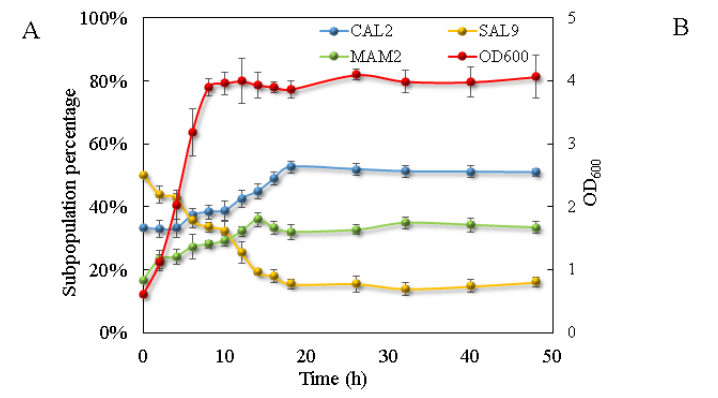


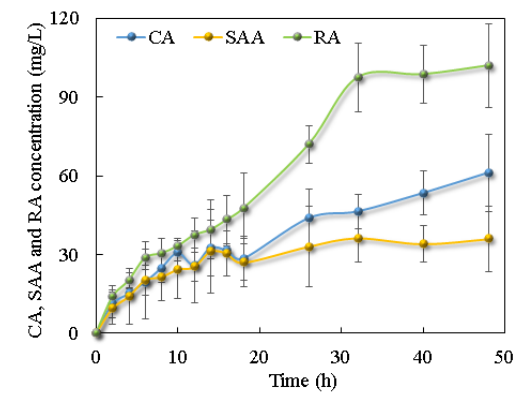


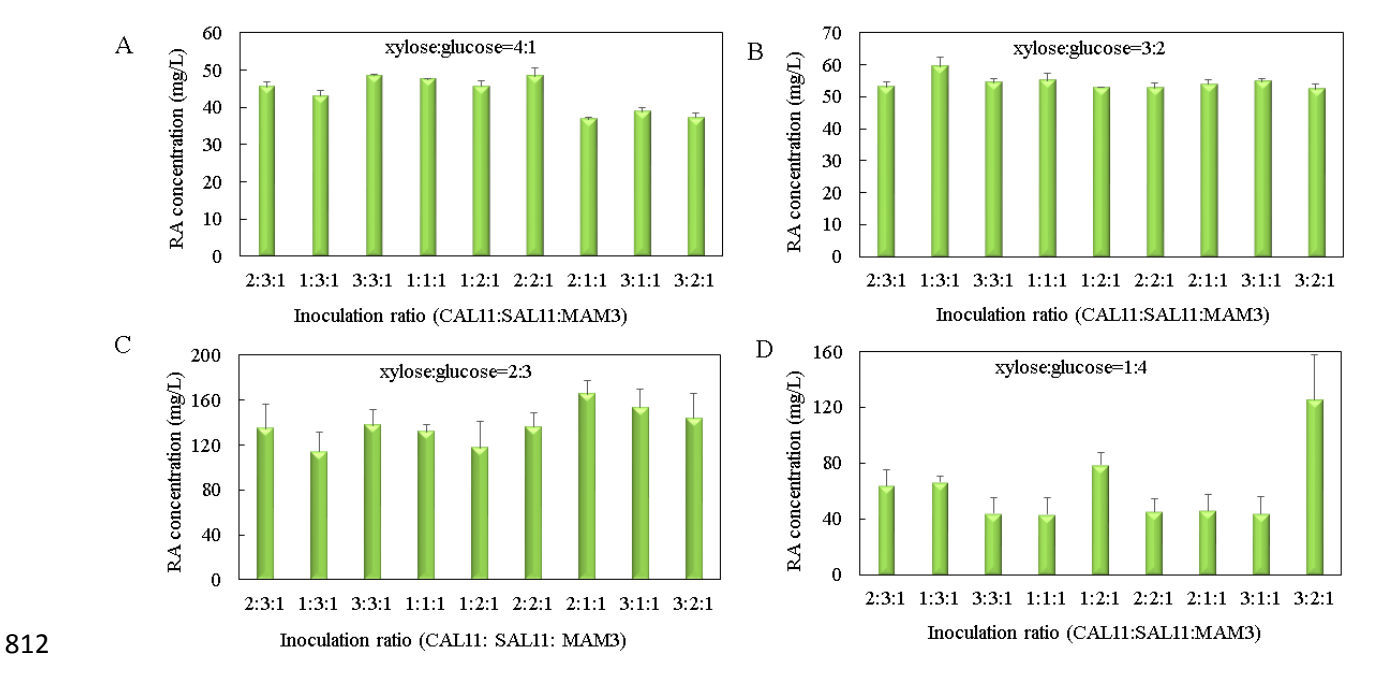


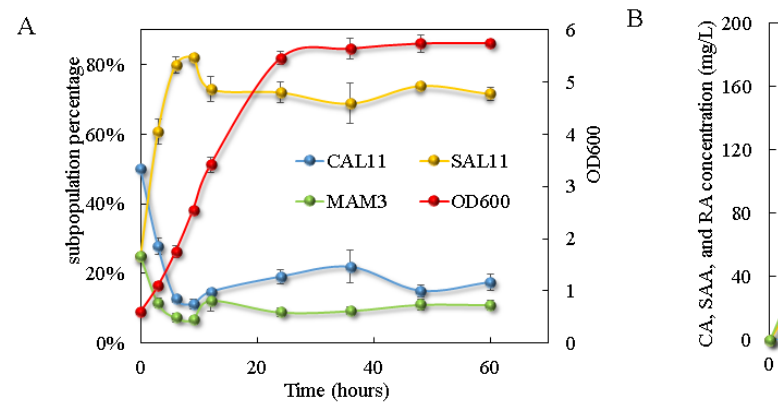


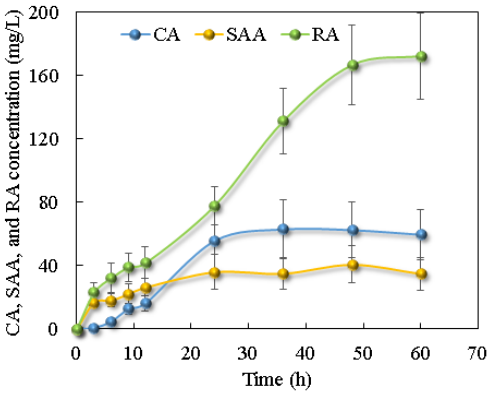
794 Figure 5











Balancing the non-linear rosmarinic acid biosynthetic pathway by modular co-culture engineering Zhenghong Li, Xiaonan Wang, Haoran Zhang Department of Chemical and Biochemical Engineering Rutgers, The State University of New Jersey 98 Brett Rd, Piscataway, NJ 08854, USA

Table S1. The DNA sequences of the primers used in this study.

Supplementary materials

ATGTCGACACTAGTATGGTTGCTGAATTGACCGCATTACG
CGAAGCTTTTACCCGCGACGCGCTTTTACT
GCCCATATGAAACCAGAAGATTTCCGCG
GACTCGAGACTAGTTTAAATCGCAGCTTCCAT
GCACTAACATATGGGTGACTGCGTTGCCCC
GCACTCGAGATACTAGTTTACTTCGGCAGGTCGCCG
ACCATATGAACAAATAGGGGTTCCGC
TGCTCGAGTTCCATTCAGGTCGAGGT
CTTATTACGCGCCTGACT
AGTCACAGGCAATAAGGC
TAATACGACTCACTATAGGG
GCCTCGAGCGACTAGTTCACGCGGACAATTCCTC

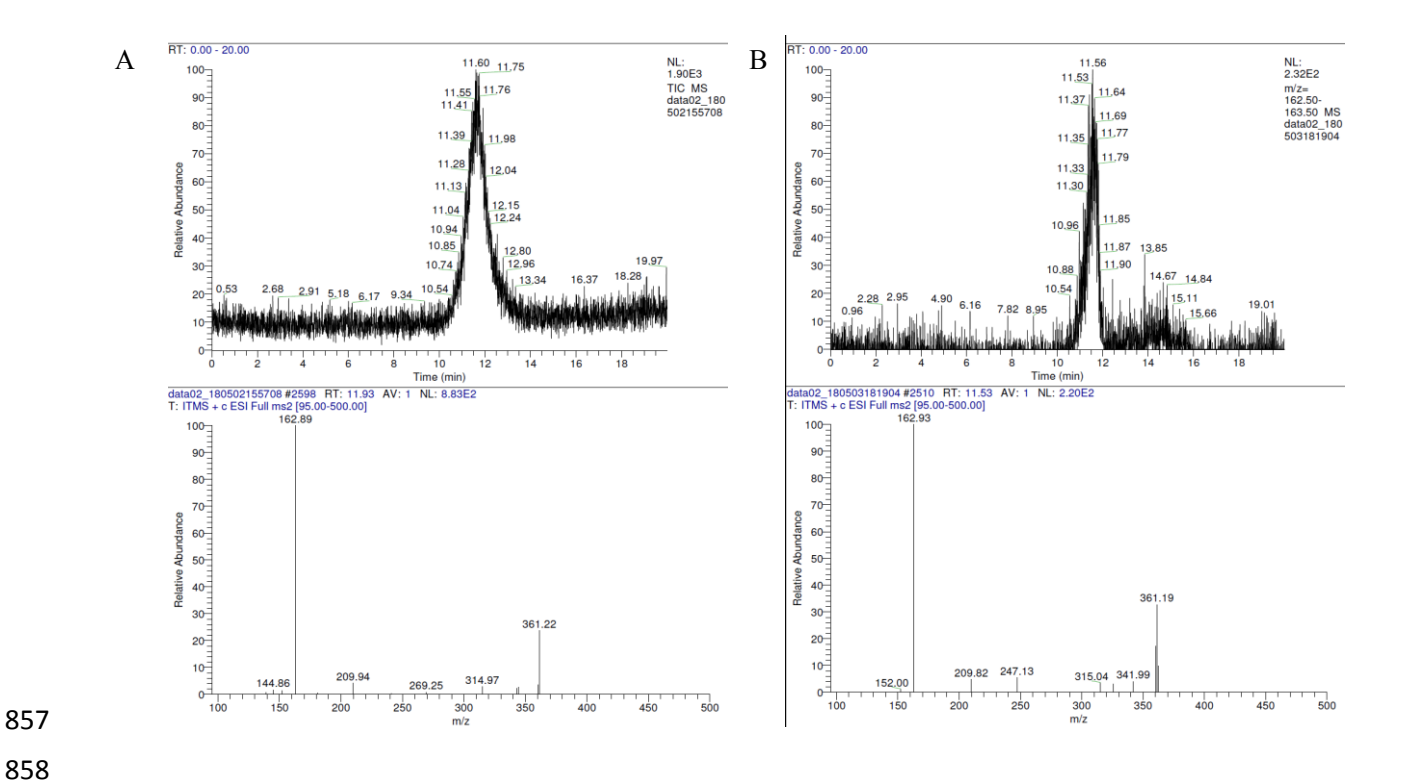


Fig. S1 Confirmation of the constructed pathway's biosynthetic activity for producing RA. (A) LC-MS/MS chromatogram and mass spectrum for the RA standard. (B) LC-MS/MS chromatogram and mass spectrum for RA produced by the engineered *E. coli* MRA containing the constructed RA biosynthesis pathway.

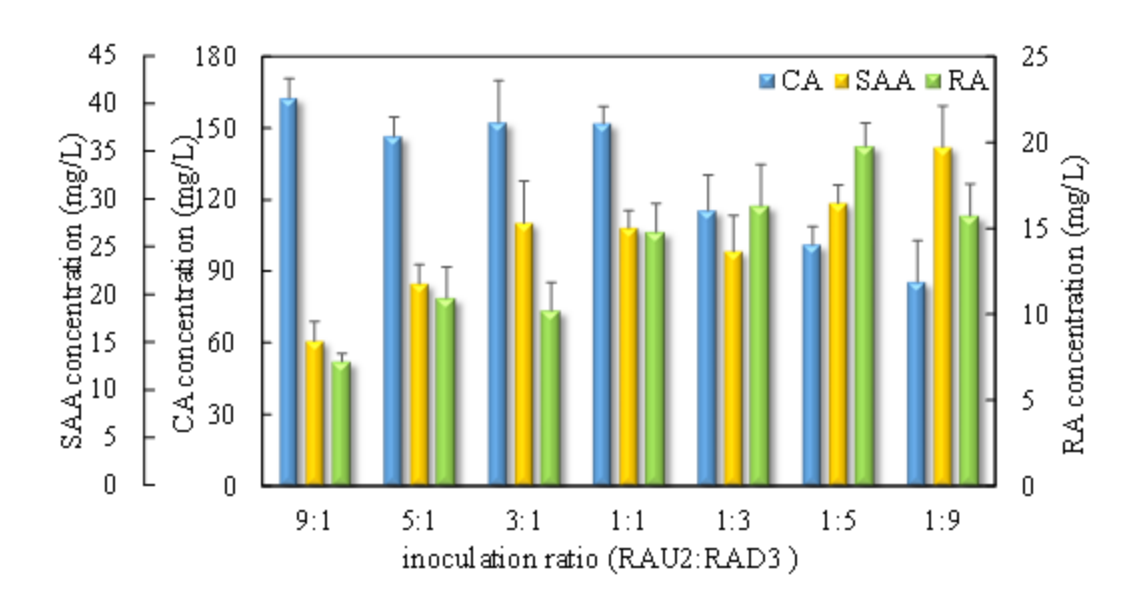
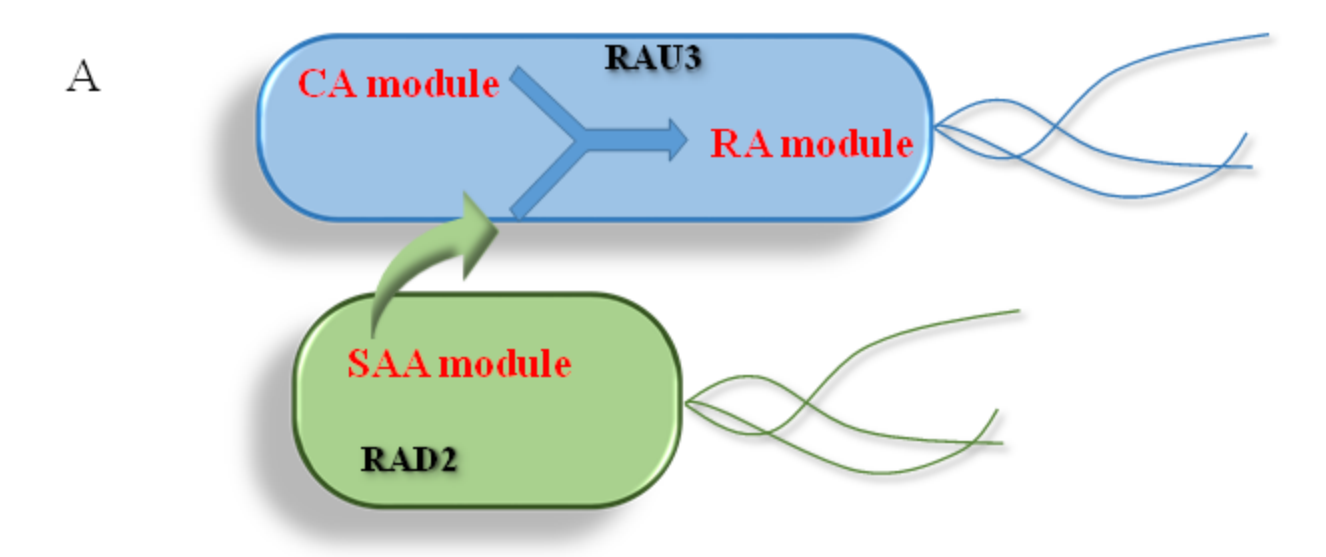


Fig. S2 The RA bioproduction by the RAU2:RAD3 co-culture at varying inoculation ratios. RAD3 is a derivative strain of *E. coli* BL21(DE3) harboring the SAA and RA modules.



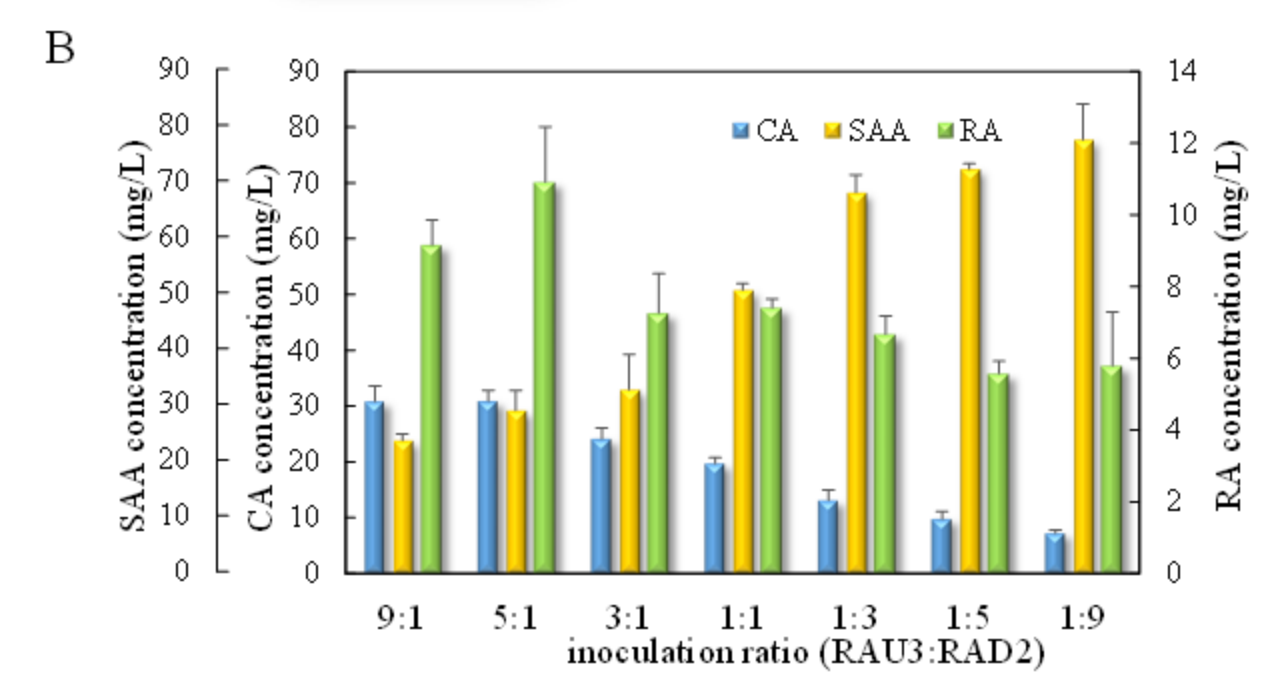


Fig. S3 An alternative two-strain co-culture for the RA biosynthesis. (A) The schematic of the co-culture design that accommodated the pathway modules. The CA and RA modules were harbored in one strain, whereas the SAA module was harbored in the other strain. (B) The RA bioproduction using the RAU3:RAD2 co-culture based on the design in (A).

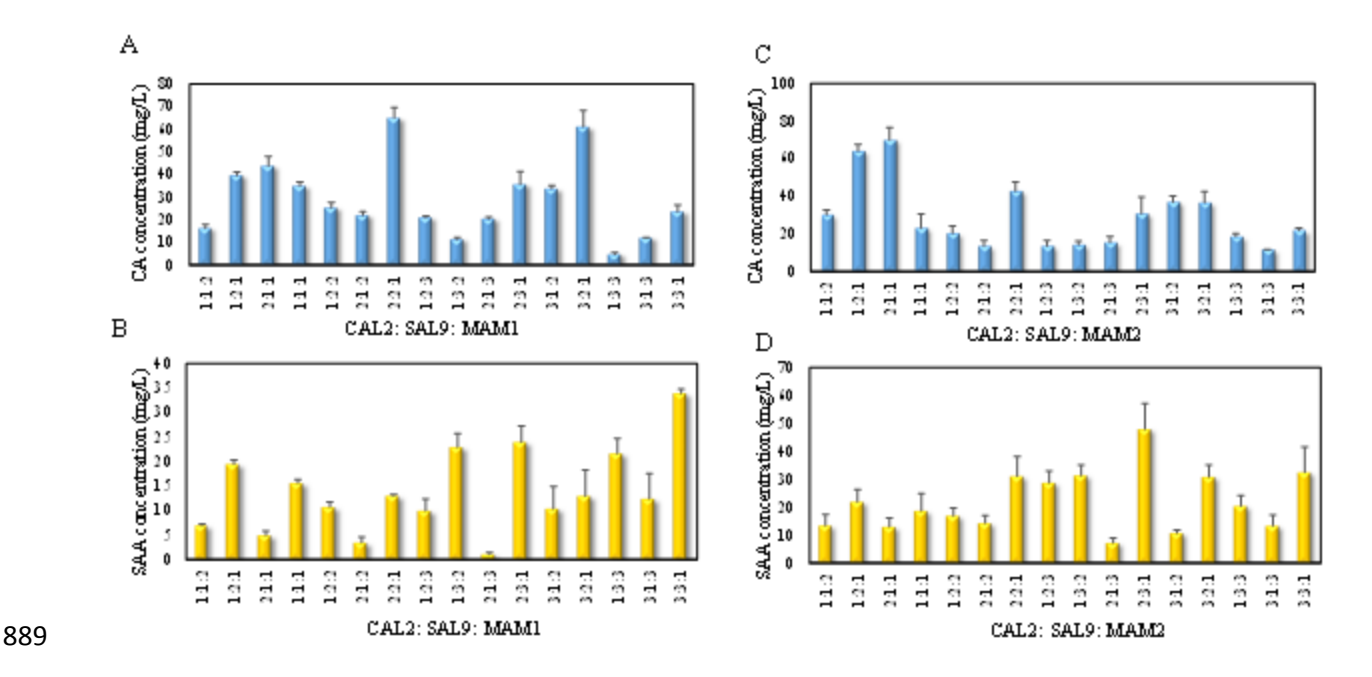


Fig. S4 The CA and SAA accumulation in the CAL2:SAL9:MAM1 and CAL2:SAL9:MAM2 co-cultures grown on glucose. (A) Concentrations of CA produced by the CAL2:SAL9:MAM1 co-culture inoculated at different ratios. (B) Concentrations of CA produced by the CAL2:SAL9:MAM2 co-culture inoculated at different ratios. (C) Concentrations of SAA produced by the CAL2:SAL9:MAM1 co-culture inoculated at different ratios. (D) Concentrations of SAA produced by the CAL2:SAL9:MAM2 co-culture inoculated at different ratios.

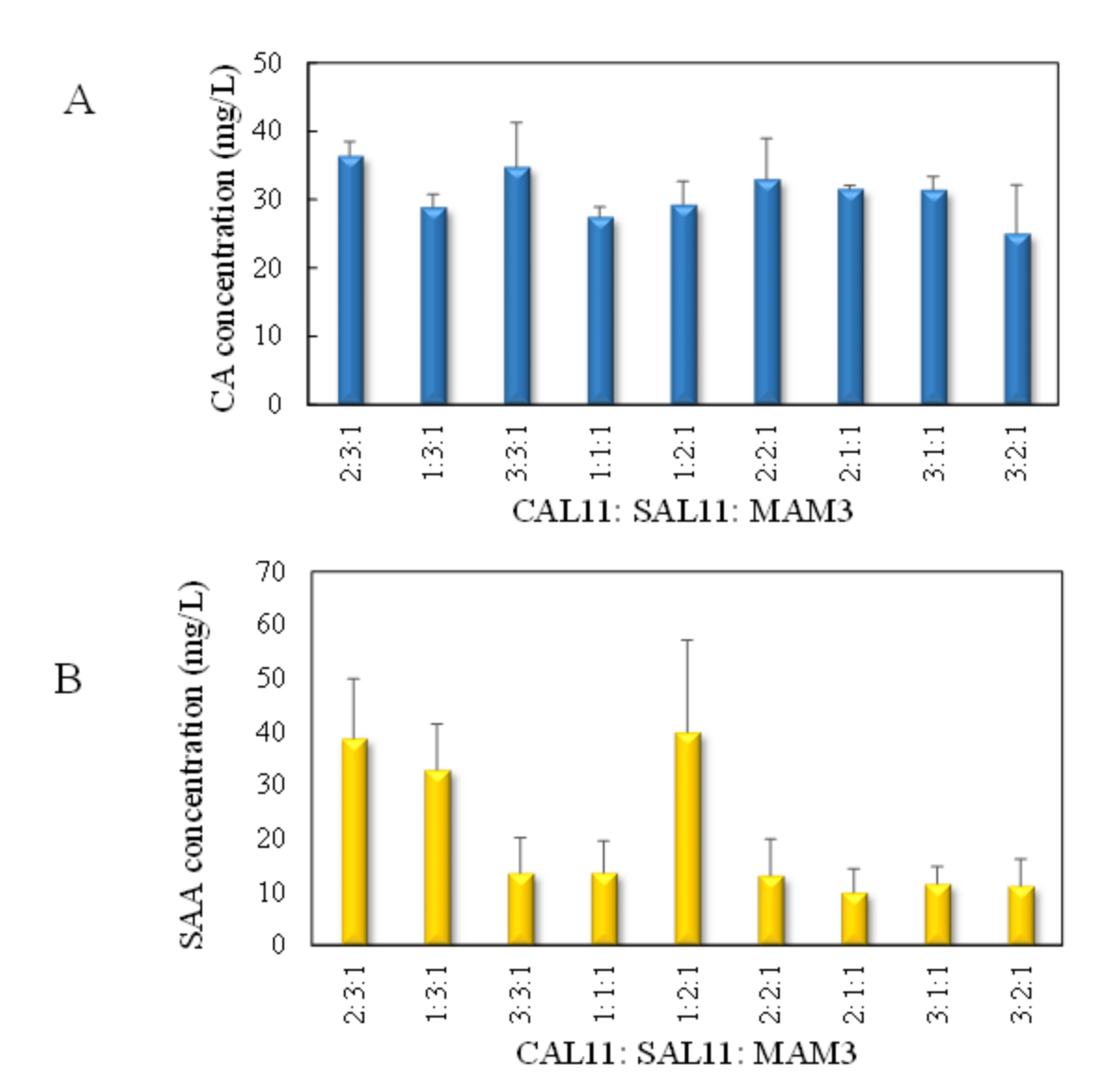


Fig. S5 The CA and SAA accumulation in the CAL11:SAL11:MAM3 co-culture grown on the mixture of 2 g/L xylose and 3 g/L glucose. (A) Concentrations of CA produced by the co-culture inoculated at different ratios. (B) Concentrations of SAA produced by the co-culture inoculated at different ratios.